Symmetry properties of the nodal superconductor $PrOs_4Sb_{12}$

T. R. Abu Alrub and S. H. Curnoe

Department of Physics and Physical Oceanography,
Memorial University of Newfoundland, St. John's, NL, A1B 3X7, Canada

We present a theoretical study of the superconducting gap function in $PrOs_4Sb_{12}$ using a symmetry-based approach. A three-component order parameter in the triplet channel best describes superconductivity. The gap function is non-degenerate and the lower branch has four cusp nodes at unusual points of the Fermi surface, which lead to power law behaviours in the density of states, specific heat and nuclear spin relaxation rate.

I. INTRODUCTION

By most accounts, $PrOs_4Sb_{12}$ is an unconventional superconductor.[1,2,3,4,5,6,7,8,9] The superconducting phase breaks time-reversal symmetry[4] and the paired electrons are in a spin triplet configuration.[9] The existence of point nodes in the superconducting gap function is indicated by power law behaviour in the temperature dependencies of specific heat,[2,8] penetration depth,[5] thermal conductivity[3], and Sb-NQR;[10] however other experiments find the gap function to be nodeless.[11,12,13] Two distinct features in the specific heat[4,14,15] and other measurements[3,5,16,17,18,19] were initially interpreted as two phase transitions involving a change in symmetry of the superconducting order parameter, but recently these results have been ascribed to sample inhomogeneity or two-band superconductivity.[20,21,22,23] On the theoretical side, several phenomenological unconventional order parameters have been proposed[24,25,26,27] and unconventional pairing mechanisms have been studied.[28,29] In light of all these intriguing and somewhat contradictory findings, it is not surprising that the only consensus on the symmetry of the superconducting order parameter is that it is probably unconventional.

In this paper, we will consider the results of a strict analysis of symmetry and symmetry-breaking described by Landau theory.[30,31,32] According to this approach, the order parameter which describes the normal to superconducting phase transition must belong to one of the irreducible representations of the crystallographic point group. Each irreducible representation yields a limited number of superconducting phases. The most convenient and accurate way to label the various phases is by their symmetry groups. All of the superconducting symmetry groups are subgroups of the normal phase symmetry $G \times U \times \mathcal{K}$, where G is the point group of the crystal, U is $U(1)$ gauge (phase) symmetry and $\mathcal{K}$ is time-reversal. Some of the subgroups include elements which are nontrivial combinations of phases, time reversal and point group elements. As described by Sigrist and Ueda[31] and Volovik and Gor'kov,[30] strong spin-orbit coupling is assumed in this classification scheme.

The point group symmetry of $PrOs_4Sb_{12}$ is T_h (tetrahedral), which has a one-dimensional representation $A_{g,u}$, a two-dimensional representation $E_{g,u}$ and a three-dimensional representation $T_{g,u}$, in each of the singlet (subscripted by g) and triplet (subscripted by u) channels. The A_g order parameter describes a "conventional" or "s-wave" superconductor. It is associated with a single, fully gapped superconducting phase. The A_u order parameter describes triplet superconductivity, also with a single, fully gapped superconducting phase. The $A_{g,u}$ phases have symmetry $T \times \mathcal{K}$, where T is the tetrahedral point group. The $E_{g,u}$ and $T_{g,u}$ order parameters are each associated with more than one superconducting phases, corresponding to different symmetries. The $E_{g,u}$ order parameters describe three different superconducting phases, of which two are accessible from the normal state via a second order phase transition, while the $T_{g,u}$ order parameters describe nine different superconducting phases, of which four are accessible from the normal state. The symmetry properties of all of these states and their corresponding gap nodes are given in Table I of Ref. 32.[34]

The order parameter which best describes experiments is T_u, the three component order parameter in the triplet channel. Broken time reversal symmetry rules out the $A_{g,u}$ order parameters. The $E_{g,u}$ phase that is accessible from the normal phase and that breaks time reversal symmetry is $T(D_2)$, which has point nodes in the $\langle 111 \rangle$ directions which are not indicated in any experiment. The T_g phases which are accessible from the normal state have either time reversal symmetry, line nodes, or nodes in the $\langle 111 \rangle$ directions, leaving T_u as the only possibility. There are two T_u phases accessible from the normal phase that break time reversal symmetry: $C_3(E)$ and $D_2(E)$; the former has nodes in the $\langle 111 \rangle$ directions, leaving the phase $D_2(E)$ as the most likely candidate. The elements of the symmetry group $D_2(E)$ are $\{E, C_2^x \mathcal{K}, U_1(\pi)C_2^y \mathcal{K}, U_1(\pi)C_2^z\}$, where E is the identity, $U_1(\pi)$ are phases, C_2^i are rotations of π about the i-axis, and $\mathcal{K}$ is time reversal. The triplet $D_2(E)$ phase has four point nodes in the $[\pm\alpha, \pm\beta, 0]$ directions. The proof that $D_2(E)$ has nodes in the triplet channel is given in the Appendix.

The issue of whether there are two different superconducting phases (as suggested by specific heat and thermal conductivity experiments[3,4,14,15,16,17]) or

only one (according to the two-band superconductivity scenario[20,21,22,23]) is to some extent by-passed by a fluke of Landau theory: the $D_2(E)$ phase is accessible via second order phase transitions both directly from the normal phase and via an intermediate phase $D_2(C_2) \times \mathcal{K}$. Thus it is a viable candidate for either situation. Therefore, we identify $D_2(C_2) \times \mathcal{K}$ as the 'A-phase' and $D_2(E)$ as the 'B-phase', and we will consider both the case when the A-phase is present and the case when the A-phase is absent on the phase diagram. Note that the elements of the group $D_2(C_2) \times \mathcal{K}$ are $\{E, C_2^x, U(\pi)C_2^y, U(\pi)C_2^z\} \times \mathcal{K}$ and that $D_2(E)$ is a subgroup of $D_2(C_2) \times \mathcal{K}$.

Recently, microscopic weak coupling theory has been applied to tetrahedral superconductors[35,36], and it was shown that the phase $D_2(C_2) \times \mathcal{K}$ is stable, while $D_2(E)$ is not.[36] This is apparently in disagreement with the observation of broken time reversal symmetry, which means either that $PrOs_4Sb_{12}$ is a strong coupling superconductor, as claimed in Refs. 13,15,19,22 or that the B-phase is better described as a $D_2(C_2) \times \mathcal{K}$ phase. We shall not pursue this possibility here, apart from noting that there are still issues whose resolution may change the conclusions of this work.

II. THE SUPERCONDUCTING GAP FUNCTION

The superconducting gap function is a 2×2 matrix in pseudospin space,

$$\widetilde{\Delta}(\boldsymbol{k}) = i\tilde{\sigma}_y \psi(\boldsymbol{k}) = \begin{pmatrix} 0 & \psi(\boldsymbol{k}) \\ -\psi(\boldsymbol{k}) & 0 \end{pmatrix} \qquad (1)$$

in the singlet channel, and

$$\widetilde{\Delta}(\boldsymbol{k}) = i[\tilde{\boldsymbol{\sigma}} \cdot \boldsymbol{d}(\boldsymbol{k})]\tilde{\sigma}_y = \begin{pmatrix} -d_x(\boldsymbol{k}) + id_y(\boldsymbol{k}) & d_z(\boldsymbol{k}) \\ d_z(\boldsymbol{k}) & d_x(\boldsymbol{k}) + id_y(\boldsymbol{k}) \end{pmatrix} \qquad (2)$$

in the triplet channel, where $\psi(\boldsymbol{k})$ and $\boldsymbol{d}(\boldsymbol{k})$ are even and odd functions of $\boldsymbol{k}$, respectively. For singlet pairing, the gap function is given by

$$\Delta(\boldsymbol{k}) = |\psi(\boldsymbol{k})|, \qquad (3)$$

while for triplet pairing the gap function may be non-degenerate,

$$\Delta_{\pm}(\boldsymbol{k}) = \left[|\boldsymbol{d}(\boldsymbol{k})|^2 \pm |\boldsymbol{q}(\boldsymbol{k})|\right]^{1/2}, \qquad (4)$$

where $\boldsymbol{q}(\boldsymbol{k}) = i\boldsymbol{d}(\boldsymbol{k}) \times \boldsymbol{d}^*(\boldsymbol{k})$. When $\boldsymbol{d}(\boldsymbol{k})$ is real $\boldsymbol{q}(\boldsymbol{k})$ vanishes and the gaps are degenerate and unitary. Otherwise, the gap is non-degenerate and the lowest energy branch has a cusp where the two branches meet.

The gap function may be expanded in terms of the basis functions for a single representation of the point group,

$$\psi(\boldsymbol{k}) = \sum_i \eta_i \psi_i(\boldsymbol{k}) \qquad (5)$$

$$\boldsymbol{d}(\boldsymbol{k}) = \sum_i \eta_i \boldsymbol{d}_i(\boldsymbol{k}) \qquad (6)$$

where $\psi_i(\boldsymbol{k})$ and $\boldsymbol{d}_i(\boldsymbol{k})$ are basis functions for even (spin-singlet) and odd (spin-triplet) representations of the point group, respectively, and η_i are components of the order parameter. For the remainder of this article we will limit our discussion to the three component order parameter in the triplet channel T_u. An appropriate set of basis functions for this representation are[32]

$$\begin{aligned} \boldsymbol{d_1} &\sim ak_y\hat{\boldsymbol{z}} + bk_z\hat{\boldsymbol{y}}, \\ \boldsymbol{d_2} &\sim ak_z\hat{\boldsymbol{x}} + bk_x\hat{\boldsymbol{z}}, \\ \boldsymbol{d_3} &\sim ak_x\hat{\boldsymbol{y}} + bk_y\hat{\boldsymbol{x}}. \end{aligned} \qquad (7)$$

where a and b are arbitrary real numbers. More general forms, which include higher orders in $\boldsymbol{k}$, are considered in the Appendix.

The phases associated with each representation are minima of the Landau potential, which is expanded in terms of the order parameter. The transformation properties of the basis functions (7) get transferred to the order parameter, and the Landau potential is constructed to be invariant under all operations of the space group, gauge transformations and time reversal. The Landau potential also determines which phases are connected by second order phase transitions. A complete analysis of the Landau potentials for the tetrahedral point group T is given in Ref. 32. The three component order parameter (η_1, η_2, η_3), defined by (6) and (7), has four phases which are accessible from the normal state by a second order phase transition, $(0, 0, 1)$, $(1, 1, 1)$, $(1, e^{2\pi i/3}, e^{-2\pi i/3})$ and $(0, i|\eta_2|, |\eta_1|)$, with symmetries $D_2(C_2) \times \mathcal{K}$, $C_3 \times \mathcal{K}$, $C_3(E)$ and $D_2(E)$ respectively. Thus the components of the order parameter in the A-phase are $(0, 0, 1)$ (or, more precisely, $(0, 0, |\eta_1|)$) and in the B-phase are $(0, i|\eta_2|, |\eta_1|)$. These statements are summarised in Table I. Different domains of each phase are obtained by permuting the components; the analysis below uses this particular choice of domain. A discussion of domains appears in Section V.

phase	normal $\rightarrow$	A	$\rightarrow$ B
OP components	$(0, 0, 0) \rightarrow$	$(0, 0, |\eta_1|)$	$\rightarrow (0, i|\eta_2|, |\eta_1|)$
symmetry group	$T_h \times U \times \mathcal{K} \rightarrow$	$D_2(C_2) \times \mathcal{K} \rightarrow$	$D_2(E)$

TABLE I: Order parameter (OP) components and symmetry group elements for the proposed normal→A→B second order phase transition sequence. Note that the A-phase can be skipped, since the B-phase is also accessible from the normal phase by a second order phase transition.

The gap function (4) in the A-phase,

$$\Delta_{\pm}(\boldsymbol{k}) = |\eta_1| \left[a^2 k_y^2 + b^2 k_x^2\right]^{1/2}, \qquad (8)$$

is unitary (degenerate) and has cusp point nodes in the [001] directions, as shown in Fig. 1a. In the B-phase, the

gap function is

$$\Delta_{\pm}(\boldsymbol{k}) = \left[(|\eta_1|^2 b^2 + |\eta_2|^2 a^2) k_x^2 + |\eta_1|^2 a^2 k_y^2 + |\eta_2|^2 b^2 k_z^2 \right.$$
$$\left. \pm 2|\eta_1||\eta_2||k_x|\sqrt{a^2 b^2 k_x^2 + a^4 k_y^2 + b^4 k_z^2} \right]^{1/2} . \quad (9)$$

In this case the gap function is non-unitary and degenerate only where $\boldsymbol{d}(\boldsymbol{k}) \times \boldsymbol{d}^*(\boldsymbol{k}) = 0$, that is, along the line $k_x = 0$. The gap has four nodes which are solutions to $\Delta_-(\boldsymbol{k}) = 0$. When $|\eta_1|^2 b^2 > |\eta_2|^2 a^2$ the nodes are found at $k_y = 0$ and $\sqrt{|\eta_1|^2 b^2 - |\eta_2|^2 a^2} k_x = \pm |\eta_2| b k_z$, shown in Figs. 1b)-1d), and when $|\eta_1|^2 b^2 < |\eta_2|^2 a^2$ they are found at $k_z = 0$ and $\sqrt{|\eta_2|^2 a^2 - |\eta_1|^2 b^2} k_x = \pm |\eta_2| b k_y$. A three dimensional rendering of the lower branch of the gap function is shown in Fig. 2.
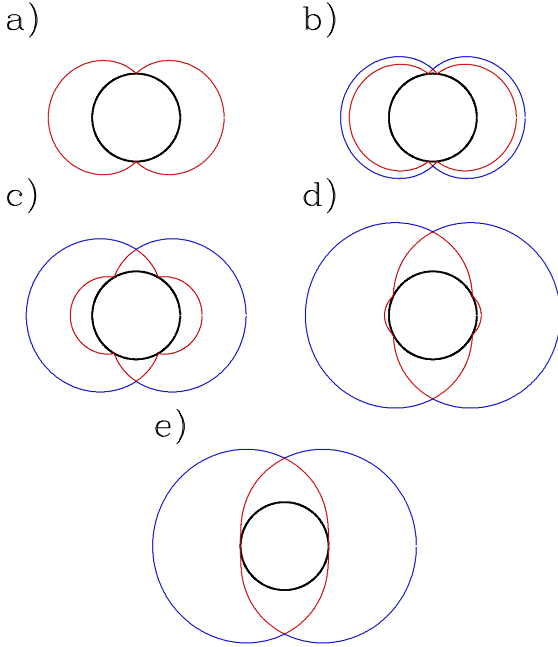

FIG. 1: (Colour) The gap function $\Delta_{\pm}(\boldsymbol{k})$ drawn over a spherical Fermi surface (bold) in the k_x-k_z plane. In a) the gap function (red) is unitary and degenerate. In b)-e) the gap function it is non-unitary and non-degenerate. The lower branch $\Delta_-(\boldsymbol{k})$ (red) and the upper branch $\Delta_+(\boldsymbol{k})$ (blue) are both shown. a) A-phase, $\eta_2 = 0$. b) B-phase, $|\eta_2|a = 0.1|\eta_1|b$. c) B-phase, $|\eta_2|a = 0.5|\eta_1|b$. d) B-phase, $|\eta_2|a = 0.9|\eta_1|b$. e) B-phase, $|\eta_2|a = |\eta_1|b$.

As discussed in the Introduction, the B-phase may evolve either from the A-phase, with $|\eta_2| \ll |\eta_1|$, or directly from the normal phase, in which case $|\eta_2| \approx |\eta_1|$. We now discuss these two scenarios in detail.

The order parameter of the A→B transition is η_2, which increases continuously from zero at the phase transition. The two degenerate cusp nodes in the [001] directions in the A-phase (Fig. 1a) split into four non-degenerate cusp nodes in the B-phase at the phase transition (Fig. 1b).
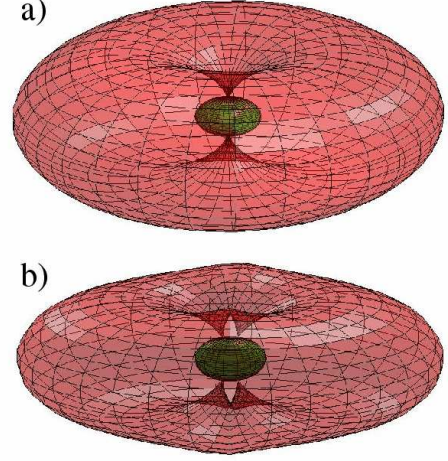

FIG. 2: (Colour) The gap function drawn over a spherical Fermi surface for the a) A-phase and b) B-phase. In a) the gap function is unitary and degenerate. In b) the gap function it is non-unitary and non-degenerate. Only the lower branch of the gap function $\Delta_-(\boldsymbol{k})$ is shown.

The order parameter of the normal→B transition is $|\eta_1| = |\eta_2|$. In this case, the B-phase resembles the $D_4(E)$ phase of octahedral systems corresponding to the three-dimensional representations with components $(0, i, 1)$. In the Landau potential, the difference between octahedral and tetrahedral appears only in sixth order and higher terms in the order parameter.[32] Near the normal-to-superconducting phase transition, when all components of the order parameter are small, the growth of the order parameter is governed by fourth order terms in the Landau potential, which are identical for octahedral and tetrahedral systems, so $|\eta_2| = |\eta_1|$ at the phase transition in both cases. The difference between the gap functions of octahedral and tetrahedral systems with 3D order parameter components $(0, i, 1)$ is due to a difference in the basis functions (7): $|a| = |b|$ in octahedral systems. Thus the octahedral phase $(0, i, 1)$ has two non-degenerate smooth nodes in the [100] directions shown in Fig. 1e), while the tetrahedral system has four cusp nodes (Figs. 1b-1d).

Thus the main difference between the two possible scenarios is the positioning of the nodes at the onset of the B-phase. In the normal→A→B scenario, the nodes will always be found in pairs near the [001] directions (Fig. 1b), while in the normal→B scenario, the positions of the four nodes are arbitrary (Fig. 1b-1d) and depend on the parameters a and b.

III. DENSITY OF STATES

The low temperature form of the density of states (DOS) in superconductors is governed by the presence of nodes.[31,37,38] In general, cusp-like point nodes give rise to a quadratic dependence on energy.

The DOS is given by[31]

$$N(\omega) = \frac{1}{(2\pi)^3} \int d^3k \sum_{\pm} \delta(\omega - E_{\pm}(\boldsymbol{k})), \qquad (10)$$

where $E_{\pm}(\boldsymbol{k}) = \sqrt{\varepsilon^2(\boldsymbol{k}) + \Delta_{\pm}^2(\boldsymbol{k})}$ and $\varepsilon(\boldsymbol{k}) = \frac{k^2}{2m} - E_F$ is the free particle energy.

A. A-phase

The gap function of the A-phase (8) is unitary and non-degenerate (Fig. 1a). Since the main contributions to the integral come from the vicinity of the nodes, the integral over $\boldsymbol{k}$ can be split into two separate regions centred over each node, which are cut off such that the total integrated region in k-space equals the Brillouin zone.[39] The nodes are degenerate and the contributions from each node are equal,

$$\begin{aligned} N(\omega) \;=\; & \frac{4v^2}{ab|\eta_1|^2(2\pi)^3} \int_0^{2\pi} d\phi \int_0^{\infty} dk_{\parallel}k_{\parallel} \\ & \int_{-\infty}^{\infty} dk_{\perp}\delta(\omega - E(k_{\parallel}, k_{\perp})) \end{aligned} \qquad (11)$$

where $k_{\parallel}$ and $k_{\perp}$ are the momenta parallel and perpendicular to the Fermi surface at the node, $v^2 k_{\parallel}^2 = |\eta_1|^2(a^2 k_y^2 + b^2 k_x^2)$, $k_{\perp} = k_z - k_F$ and $E(k_{\parallel}, k_{\perp}) \approx \sqrt{k_{\perp}^2 v_F^2 + k_{\parallel}^2 v^2}$. Changing variables again and using $p_1 = v_F k_{\perp} = p \cos\theta$, $p_2 = v\, k_{\parallel} = p \sin\theta$, we find

$$\begin{aligned} N(\omega) \;=\; & \frac{4}{ab|\eta_1|^2(2\pi)^2 v_F} \int_0^{\infty} dp_2 p_2 \int_{-\infty}^{\infty} dp_1 \delta(\omega - E(p_1, p_2)) \\ \;=\; & \frac{4}{ab|\eta_1|^2(2\pi)^2 v_F} \int_0^{\pi} \sin\theta d\theta \int_0^{p_0} dp\, p^2 \delta(\omega - p) \quad (12) \\ \;=\; & \frac{2\omega^2}{ab|\eta_1|^2\pi^2 v_F} \end{aligned} \qquad (13)$$

where the cutoff p_0 is finally introduced in the last equation. This result is equivalent to the usual result for a degenerate cusp node, $N(\omega) = \omega^2/\pi^2 v_F v_g^2$,[38] apart from a factor of two because there are two degenerate nodes in our calculation. In our case, the gap velocity, defined by $\boldsymbol{v}_g = \boldsymbol{\nabla}_{\boldsymbol{k}}\Delta(\boldsymbol{k})$ is not the same in all directions since the node is not rotationally symmetric, and so the geometric average $\bar{v}_g = |\eta_1|(ab)^{1/2}$ appears.

Eq. 13 is the density of states of the phase $(0,0,1)$ $(D_2(C_2) \times \mathcal{K})$ at low temperatures. However, according to the considerations outlined in Section I, this phase is identified as the A-phase, which is only found in a narrow region of phase space just below H_{c2}. Therefore, Eq. 13 is not expected to be observed in PrOs$_4$Sb$_{12}$.

B. B-Phase

In triplet, non-unitary phases, in general, the gap function is non-degenerate, except along some lines on the Fermi surface. All nodes are found in the lower energy branch of the gap function Δ_-, and the higher energy branch Δ_+ is usually neglected. However, if the nodes are found near the line where the gaps are degenerate then both gaps should be taken into account.

To find the density of states in the B-phase, we should consider the two different scenarios, normal→A-phase→B-phase or normal→B-phase, separately. In the former scenario, $|\eta_2| \ll |\eta_1|$, and pairs of nodes are found on opposite sides of the Fermi surface. The partners in each pair are very close to each other and close to the gap degeneracy line, as shown in Fig. 1b). In this case, the higher energy gap should not be neglected. In the normal→B-phase scenario, the positions of the nodes depend on the parameters a and b which are arbitrary.

1. normal→A-phase→B-phase

At the onset of the B-phase $|\eta_2| \ll |\eta_1|$, and we will assume that $|\eta_1|^2 b^2 > |\eta_2|^2 a^2$. Then the pairs of nodes are found in the vicinity of [001] in the plane $k_y = 0$, as shown in Fig. 1b). The integration over k-space is divided into four regions, which overlap for nodes within a pair.

The gap function in the vicinity of the nodes for the case when $|\eta_1|^2 b^2 > |\eta_2|^2 a^2$ can be approximated by

$$\Delta(\boldsymbol{k}) \approx \sqrt{|\eta_1|^2 b^2 - |\eta_2|^2 a^2}\sqrt{k_{\parallel}'^2 + k_y'^2} \qquad (14)$$

where $k_y' = \frac{a}{b} k_y$ and

$$k_{\parallel}' = \frac{\sqrt{|\eta_1|^2 b^2 - |\eta_2|^2 a^2}}{|\eta_1|b}k_x \pm \frac{|\eta_2|a}{|\eta_1|b}k_z. \qquad (15)$$

With this approximation, the '−' branch of the gap function continues smoothly to the '+' branch of the gap function at the line where the gap function is degenerate. Then two difficulties are overcome at once: both branches of the gap function are taken into account, and the contributions from each integration region are distinct, even though the regions overlap. Each region yields the same contribution to the density of states,

$$N(\omega) = \frac{4}{(2\pi)^3} \frac{b}{a} \frac{v^2}{|\eta_1|^2 b^2 - |\eta_2|^2 a^2} \int_0^{2\pi} d\phi \int_0^\infty dk_{||} k_{||} \int_{-\infty}^\infty dk_\perp \delta(\omega - E(k_{||}, k_\perp)) \qquad (16)$$

where $v^2 k_{||}^2 = (|\eta_1|^2 b^2 - |\eta_2|^2 a^2)(k_{||}'^2 + k_y'^2)$, $k_\perp = \frac{\sqrt{|\eta_1|^2 b^2 - |\eta_2|^2 a^2}}{|\eta_1| b} k_z \mp \frac{|\eta_2| a}{|\eta_1| b} k_x$ and $E(k_{||}, k_\perp) \approx \sqrt{k_\perp^2 v_F^2 + k_{||}^2 v^2}$ as before. Then performing the same change of variables as in the A-phase calculation, we find

$$N(\omega) = \frac{b}{a} \frac{2\omega^2}{\pi^2 v_F(|\eta_1|^2 b^2 - |\eta_2|^2 a^2)} \qquad (17)$$

Note that in the limit $|\eta_2| \to 0$ we recover the A-phase result, as expected.

2. normal → B-phase

In this situation, near the phase transition we have $|\eta_1| \approx |\eta_2|$, however the positions of the nodes depend on the parameters a and b, which are completely undetermined. Then there are three possibilities to consider. The first is shown in Fig. 1b), where the nodes appear in pairs such that the pairs are close to the gap degeneracy line (if $|a| \ll |b|$ or $|b| \ll |a|$); in this case the above calculation is valid and the result (17) is obtained for $|\eta_1| \approx |\eta_2|$,

$$N(\omega) = \frac{b}{a} \frac{2\omega^2}{\pi^2 v_F |\eta_1|^2 (b^2 - a^2)}. \qquad (18)$$

Second, when all four nodes are spaced far apart as shown in Fig. 1c), then the above calculations are again valid and the result (18) is obtained.

Finally, the nodes may appear in pairs which are far away from the gap degeneracy line, as shown in Fig. 1d). In this case the above treatment is invalid. Here we have a crossover between $N(\omega) \sim \omega^2$ and $N(\omega) \sim |\omega|$, which is the behaviour of the limiting case shown in Fig. 1e), i.e., the octahedral phase $(0, i, 1)$, with smooth (quadratic) nodes. Such behaviour is not observed in experiments, which could mean that either the components of the order parameter are unequal (normal→A-phase→B-phase scenario) or $a \neq b$.

IV. SPECIFIC HEAT AND NUCLEAR SPIN RELAXATION RATE

The specific heat at low temperatures is given by[31]

$$C(T) = \frac{2}{T} \int_0^\infty d\omega\, \omega^2 N(\omega) \left[-\frac{\partial f}{\partial \omega} \right] \qquad (19)$$

Eqs. 13 and 17 yield

$$C(T) = \frac{14\,\pi^2}{15 v_F a b |\eta_1|^2} T^3 \qquad (20)$$

for the A-phase, and

$$C(T) = \frac{b}{a} \frac{14\,\pi^2}{15 v_F(|\eta_1|^2 b^2 - |\eta_2|^2 a^2)} T^3 \qquad (21)$$

for the B-phase.

The longitudinal nuclear spin-lattice relaxation rate is given by[31]

$$\frac{(1/T_1)_T}{(1/T_1)_{T_c}} = 2\frac{T}{T_c} \int_0^\infty d\omega\, N(\omega)N(\omega - \omega_0) \left[-\frac{\partial f}{\partial \omega} \right]. \qquad (22)$$

In the limit of small nuclear resonance frequency ω_0, one finds

$$\frac{(1/T_1)_T}{(1/T_1)_{T_c}} = \frac{28}{15\,\pi^4 v_F^2 a^2 b^2 |\eta_1|^4} \frac{T^5}{T_c} \qquad (23)$$

in the A-phase, while in the B-phase it is

$$\frac{(1/T_1)_T}{(1/T_1)_{T_c}} = \frac{b^2}{a^2} \frac{28}{15\,\pi^4 v_F^2(|\eta_1|^2 b^2 - |\eta_2|^2 a^2)^2} \frac{T^5}{T_c}. \qquad (24)$$

These expressions give the low temperature behaviour of the specific heat and nuclear relaxation rate in terms of the tetrahedral parameters a and b and the order parameter components η_1 and η_2.

V. DOMAINS

Directional dependent measurements are the ideal way to observe the anisotropy of the gap function. However, such measurements may be confounded by the presence of domains, different regions in space where the components of the order parameter are interchanged. In this section we offer a brief discussion of domains for the A-phase and the B-phase.

The A-phase has three different domains $(1, 0, 0)$, $(0, 1, 0)$ and $(0, 0, 1)$, which, in the absence of unusual crystal shape or external fields, are all expected to be present, and will lead to the observation of the full tetrahedral symmetry. Six (degenerate) nodes will be observed in the directions $\langle 00 \pm 1 \rangle$. Now let us suppose that there is some kind of external effect along the z-axis which effectively lowers the symmetry from T_h to D_{2h}. In an octahedral system, either the single domain $(0, 0, 1)$, with nodes in the $[00 \pm 1]$ directions will be favoured,

or the other two domains, $(1,0,0)$ and $(0,1,0)$ will be favoured. In the latter case, four nodes would be observed in the directions $[\pm100]$ and $[0\pm10]$. However, because the crystal symmetry of $PrOs_4Sb_{12}$ is tetrahedral to begin with, any axial perturbation will lift the degeneracy of all three domains, any of which could be favoured. Therefore, in the A-phase, if all domains are present then tetrahedral symmetry with six nodes will be observed. Otherwise, only one domain is present, the symmetry will be $D_2(C_2)$, with two nodes. It is not likely that two out of three domains would be present in the A-phase, but could be possible if they were very close in energy.

The same arguments also hold for the more complicated B-phase. Six domains are possible, with twenty-four non-degenerate nodes. If there is a single domain, then the symmetry is $D_2(E)$, and four nodes will be present.

VI. CONCLUSIONS

In this article, we have attempted to give a physical description and comparison of the sequences of phase transitions normal$\to D_2(C_2) \times \mathcal{K} \to D_2(E)$ and normal$\to D_2(E)$, which we identify with the phase transitions seen in experiments, normal$\to$A$\to$B or normal$\to$B, respectively. Although this description is derived entirely from basic considerations of symmetry, a complicated gap structure emerges with several unusual features. First, the positions of the nodes in the B-phase are not located on any symmetry axes. Although this is allowed by symmetry to occur in crystals with other point groups, such a feature has never before been considered. Second, because the B-phase is triplet and non-unitary, there are two non-degenerate gaps. The only known example of this is Sr_2RuO_4, but in that case the two gaps remain close in energy.[40] In $PrOs_4Sb_{12}$, for a direct normal$\to$B transition, the energy difference is expected to be large. Finally, the proposed A$\to$B transition, which is characterised by the splitting into two of the degenerate nodes of the the A-phase, is highly unusual.

In summary, we have proposed phase transition sequences in accordance with experimental evidence available to date and studied its basic properties. Superconductivity is best-described by a three component order parameter in the triplet channel. The superconducting phase has $D_2(E)$ symmetry, is non-unitary, and has four cusp nodes at unusual points on the Fermi surface. The presence of nodes leads to a quadratic dependence on energy in the density of states, and power law behaviour in the specific heat and nuclear spin relaxation rate. There is also a second, higher energy, nodeless gap which may be experimentally accessible.

APPENDIX A: PROOF OF THE EXISTENCE OF NODES IN THE $D_2(E)$ PHASE IN THE TRIPLET CHANNEL

In Section II, we found the gap function using basis functions given by (7), and order parameter components $(0, i|\eta_2|, |\eta_1|)$. The gap function takes the form (9), which vanishes either in the plane $k_y = 0$ at the points defined by $\sqrt{|\eta_1|^2b^2 - |\eta_2|^2a^2}k_x = \pm|\eta_2|bk_z$ when $|\eta_1|^2b^2 > |\eta_2|^2a^2$, or in the plane $k_z = 0$ at the points $\sqrt{|\eta_2|^2a^2 - |\eta_1|^2b^2}k_x = \pm|\eta_2|bk_y$ when $|\eta_1|^2b^2 < |\eta_2|^2a^2$. In Section II, only p-wave pairing (basis functions linear in $\boldsymbol{k}$) was considered. In order to rigorously demonstrate the existence of nodes all possible higher order pairings must be included in the basis functions. We now consider this most general case.

The most general form for the basis functions of the representation T in T_h is

$$
\begin{aligned}
d_1 &= (f(k_x,k_y,k_z), g(k_x,k_y,k_z), h(k_x,k_y,k_z)) \,(A1)\\
d_2 &= (h(k_y,k_z,k_x), f(k_y,k_z,k_x), g(k_y,k_z,k_x)) \,(A2)\\
&= (h', f', g')\\
d_3 &= (g(k_z,k_x,k_y), h(k_z,k_x,k_y), f(k_z,k_x,k_y) \,(A3)\\
&= (g'', h'', f'')
\end{aligned}
$$

where $f(\boldsymbol{k})$ is odd in $\boldsymbol{k}$, $g(k_x,k_y,k_z)$ is odd in k_z and even in k_x and k_y, and $h(k_x,k_y,k_z)$ is odd in k_y and even in k_x and k_z. Eventually, we will find solutions to $\Delta_-(\boldsymbol{k}) = 0$ where one of the k's is zero (in agreement with the particular case of lowest order in k basis functions (7)), so we set $f(\boldsymbol{k}) = 0$ now.

Using (4), (6) and (A1-A3) one finds

$$
\begin{aligned}
\Delta_-^2 &= |\eta_1|^2(g''^2 + h''^2) + |\eta_2|^2(g'^2 + h'^2)\\
&\quad -2|\eta_1||\eta_2|\sqrt{h''^2g'^2 + g''^2g'^2 + h''^2h'^2}. \,(A4)
\end{aligned}
$$

Case 1: $k_y = 0$: g'' vanishes and

$$
\Delta_-^2 = (|\eta_1|h'' - |\eta_2|\sqrt{g'^2 + h'^2})^2. \qquad (A5)
$$

Nodes are found where $\Delta_- = 0$, or where the function

$$
\phi_1(k_x,k_z) = h^2(k_z,k_x,0) - \frac{|\eta_2|^2}{|\eta_1|^2}(g^2(0,k_z,k_x)+h^2(0,k_z,k_x))
$$
$$(A6)$$

vanishes.
Case 2: $k_z = 0$: h' vanishes and

$$
\Delta_-^2 = (|\eta_2|g' - |\eta_1|\sqrt{g''^2 + h''^2})^2. \qquad (A7)
$$

Nodes are found where $\Delta_- = 0$, or where the function

$$\phi_2(k_x, k_y) = \frac{|\eta_2|^2}{|\eta_1|^2} g^2(k_y, 0, k_x) - (g^2(0, k_x, k_y) + h^2(0, k_x, k_y))$$

$$(A8)$$

vanishes.

We have

$$\phi_1(k_x, 0) = h^2(0, k_x, 0) - \frac{|\eta_2|^2}{|\eta_1|^2} g^2(0, 0, k_x)$$

$$\phi_1(0, k_z) = -\frac{|\eta_2|^2}{|\eta_1|^2} h^2(0, k_z, 0) < 0$$

$$\phi_2(k_x, 0) = \frac{|\eta_2|^2}{|\eta_1|^2} g^2(0, 0, k_x) - h^2(0, k_x, 0)$$

$$= -\phi_1(k_x, 0)$$

$$\phi_2(0, k_y) = -g^2(0, 0, k_y) < 0$$

If $\phi_1(k_x, 0) > 0$, then $\phi_1(k_x, k_z)$ changes sign, *i.e.*, there is a node of Δ_- in the $k_y = 0$ plane somewhere between the positions $(k_x, 0, 0)$ and $(0, 0, k_z)$. Symmetry requires that there be (at least) four nodes on the Fermi surface. If $\phi_1(k_x, 0) < 0$, then $\phi_2(k_x, k_y)$ changes sign, *i.e.*, there are four nodes in the $k_z = 0$ plane.

Thus we have proved that, in general, the triplet phase with order parameter components $(0, i|\eta_2|, |\eta_1|)$ has four nodes in either the plane $k_y = 0$ or $k_z = 0$ at the positions $[\pm\alpha, 0, \pm\beta]$ or $[\pm\alpha, \pm\beta, 0]$, where α and β depend on the particular form of the basis functions. These nodes are "approximate", in the sense that they are a consequence of symmetry and follow from the most general basis functions for the T representation. These nodes are also "rigorous", since the state $(0, i|\eta_2|, |\eta_1|)$ couples to no secondary superconducting order parameters.[32]

[1] M. B. Maple, E. D. Bauer, V. S. Zapf, E. J. Freeman, N. A. Frederick and R. P. Dickey, Acta. Phys. Pol. **32**, 3291 (2001).

[2] E. D. Bauer, N. A. Frederick, P.-C. Ho, V. S. Zapf, and M. B. Maple, Phys. Rev. B **65**, 100506(R) (2002).

[3] K. Izawa, Y. Nakajima, J. Goryo, Y. Matsuda, S. Osaki, H. Sugawara, H. Sato, P. Thalmeier, and K. Maki, Phys. Rev. Lett. **90**, 117001 (2003).

[4] Y. Aoki, A. Tsuchiya, T. Kanayama, S. R. Saha, H. Sugawara, H. Sato, W. Higemoto, A. Koda, K. Ohishi, K. Nishiyama, and R. Kadono, Phys. Rev. Lett. **91**, 067003 (2003).

[5] E. E. M. Chia, M. B. Salamon, H. Sugawara, and H. Sato, Phys. Rev. Lett. **91**, 247003 (2003).

[6] A. D. Huxley, M.-A. Measson, K. Izawa, C. D. Dewhurst, R. Cubitt, B. Grenier, H. Sugawara, J. Flouquet, Y. Matsuda and H. Sato, Phys. Rev. Lett. **93**, 187005 (2004).

[7] M. Nishiyama, T. Kato, H. Sugawara, D. Kikuchi, H. Sato, H. Harima, and G.-q. Zheng, J. Phys. Soc. Jpn. **74**, 1938 (2005).

[8] N. A. Frederick, T. A. Sayles and M. B. Maple, Phys. Rev. B **71**, 064508 (2005).

[9] W. Higemoto, S. R. Saha, A. Koda, K. Ohishi, R. Kadono, Y. Aoki, H. Sugawara and H. Sato, Phys. Rev. B **75**, 020510(R) (2007).

[10] K. Katayama, S. Kawasaki, M. Nishiyama, H. Sugawara, D. Kikuchi, H. Sato, and G.-q. Zheng, J. Phys. Soc. Jpn. **76**, 023701 (2007).

[11] D. E. MacLaughlin, J. E. Sonier, R. H. Heffner, O. O. Bernal, B.-L. Young, M. S. Rose, G. D. Morris, E. D. Bauer, T. D. Do and M. B. Maple, Phys. Rev. Lett. **89**, 157001 (2002).

[12] H. Suderow, S. Viera, J. D. Strand, S. Bud'ko and P. C. Canfield, Phys. Rev. B **69**, 060504 (2004).

[13] H. Kotegawa, M. Yogi, Y. Imamura, Y. Kawasaki, G.-q. Zheng, Y. Kitaoka, S. Ohsaki, H. Sugawara, Y. Aoki, and H. Sato, Phys. Rev. Lett. **90**, 027001 (2003).

[14] Y. Aoki, T. Namiki, S. Ohsaki, S. R. Saha, H. Sugawara and H. Sato, J. Phys. Soc. Jpn. **71**, 2098 (2002).

[15] R. Vollmer, A. Faiβt, C. Pfleiderer, H. v. Löhneysen, E. D. Bauer, P.-C. Ho, V. Zapf, and M. B. Maple, Phys. Rev. Lett. **90**, 057001 (2003).

[16] T. Tayama, T. Sakakibara, H. Sugawara, Y. Aoki and H. Sato, J. Phys. Soc. Jpn. **72**, 1516 (2003).

[17] P.-C. Ho, N. A. Frederick, V. S. Zapf, E. D. Bauer, T. D. Do, M. B. Maple, A. D. Christianson, and A. H. Lacerda, Phys. Rev. B **67**, 180508(R) (2003).

[18] N. Oeschler, P. Gegenwart, F. Weickert, I. Zerec, P. Thalmeier, F. Steglich, E. D. Bauer, N. A. Frederick and M. B. Maple, Phys. Rev. B **69**, 235108 (2004).

[19] K. Grube, S. Drobnik, C. Pfleiderer, H. v. Löhneysen, E. D. Bauer and M. B. Maple, Phys. Rev. B **73**, 104503 (2006).

[20] M.-A. Measson, D. Braithewaite, J. Flouquet, G. Seyfarth, J. P. Brison, E. Lhotel, C. Paulsen, H. Sugawara and H. Sato, Phys. Rev. B **70**, 064516 (2004).

[21] G. Seyfarth, J. P. Brison, M.-A. Measson, J. Flouquet, K. Izawa, Y. Matsuda, H. Sugawara, and H. Sato, Phys. Rev. Lett. **95**, 107004 (2005).

[22] G. Seyfarth, J. P. Brison, M.-A. Méasson, D. Braithewaite, G. Lapertot and J. Flouquet, Phys. Rev. Lett. **97**, 236403 (2006).

[23] M. Yogi, T. Nagai, Y. Imamura, H. Mukuda, Y. Kitaoka, D. Kikuchi, H. Sugawara, Y. Aoki, H. Sato and H. Harima, J. Phys. Soc. Jpn. **75**, 124702 (2006).

[24] J. Goryo, Phys. Rev. B **67**, 184511 (2003).

[25] M. Ichioka, N. Nakai and K. Machida, J. Phys. Soc. Jpn. **72**, 1322 (2003).

[26] K. Miyake, H. Kohno and H. Harima, J. Phys.: Condens. Matter **15**, L275 (2003).

[27] K. Maki, S. Haas, D. Parker, H. Won, K. Izawa and Y. Matsuda, Europhys. Lett. **68**, 720 (2004).

[28] M. Matsumoto and M. Koga, J. Phys. Jpn. **73**, 1135 (2004); M. Matsumoto and M. Koga, J. Phys. Jpn. **74**, 1686 (2005); M. Koga, M. Matsumoto and H. Shiba, J. Phys. Soc. Jpn. **75**, 014709 (2006).

[29] P. Thalmeier, Physica B **378-380**, 261 (2006).

[30] G. E. Volovik and L. P. Gor'kov, Sov. Phys. JETP **61**, 843 (1985); Yu. M. Gufan, JETP **80**, 485 (1995).

[31] M. Sigrist, and K. Ueda, Rev. Mod. Phys., **63**, 239 (1991)

[32] I. A. Sergienko and S. H. Curnoe, Phys. Rev. B, **70**, 144522 (2004); see Ref. 34.

[33] S. H. Curnoe, T. R. Abu Alrub, I. A. Sergienko and I. Vekhter, J. Magn. Magn. Mater. **310**, 605 (2007).

[34] There is an error in Table I of Ref. [32]. The triplet-paired phase with symmetry $D_2(E)$ was reported to be nodeless. However, it does in fact have four point nodes (approximate and rigorous) at the positions $[\pm\alpha, \pm\beta, 0]$. This result can be proved rigorously as a strict consequence of symmetry (see Appendix A). This error lead to our claim [33] that the nodes lift away from the Fermi surface to form deep dips in the gap function at the A-B transition.

[35] V. Kuznetsova and V. Barzykin, Europhys. Lett. **72** (3), 437 (2005).

[36] S. Mukherjee and D. F. Agterberg, Phys. Rev. B **74**, 174505 (2006).

[37] Yu. S. Barash, and A. A. Svidzinsky, Phys. Rev. B, **53**, 15254 (1996).

[38] R. Joynt, and L. Taillefer, Rev. Mod. Phys. **74**, 235 (2002).

[39] A. C. Durst and P. A. Lee, Phys. Rev. B **62** 1270 (2000).

[40] A. P. Mackenzie and Y. Maeno, Rev. Mod. Phys. **75**, 657 (2003).